



PERGAMON

Available online at www.sciencedirect.com

SCIENCE @ DIRECT®

Polyhedron 22 (2003) 2125–2131



POLYHEDRON

www.elsevier.com/locate/poly

Two applications of metal cyanide square grid monolayers: studies of evolving magnetic properties in layered films and templating Prussian blue family thin films

Jeffrey T. Culp^a, Ju-Hyun Park^b, Isa O. Benitez^a, Mark W. Meisel^b,
Daniel R. Talham^{a,*}

^a Department of Chemistry, University of Florida, Gainesville, FL 32611-7200, USA

^b Department of Physics and Center for Condensed Matter Sciences, University of Florida, Gainesville, FL 32611-8440, USA

Received 6 October 2002; accepted 14 January 2003

Abstract

Two applications of previously described square grid network monolayers prepared at the air/water interface are explored. The monolayer networks are single layers of Prussian blue like mixed-metal cyanide networks that are formed via the interface-directed condensation of amphiphilic pentacyanometallate complex and subphase metal ions. In the first application, the monolayers are deposited onto solid supports and the magnetic properties of the networks are evaluated, as the transferred films evolve from a monolayer to a bilayer to multilayers. In the second application, the network monolayers are used to derivatize a surface, providing a seed layer for the subsequent deposition of solid-state metal cyanide molecule-based magnets. Improved surface wetting results in continuous, transparent magnetic films.

© 2003 Elsevier Science Ltd. All rights reserved.

Keywords: Magnetic properties; Pentacyanoferrate complexes; Square grid network; Magnetometry

1. Introduction

While there have been impressive recent advances in supramolecular synthesis, many of the technological applications of nanometer-scale objects are likely to also require positioning the structures at surfaces. Future generations of electronics and information storage architectures, often cited as motivation for nanoscale fabrication, will likely still be fabricated onto a solid support. An attractive alternative to the multistep process of synthesis and isolation, followed by deposition, would be to fabricate the nanoscale objects directly at the site of use. Therefore, there is a significant need to investigate supramolecular assembly at a surface or interface, and this need certainly extends to molecule-based magnets. With a growing understanding of how to synthesize supramolecular magnetic materials, we are

now in position to study how the requirements of such assembly processes change when performed at an interface and how the magnetic response of the materials are influenced.

Our studies of assembly at interfaces have focused on the air/water interface [1]. An air/liquid interface eliminates many obstacles inherent to carrying out reactions at surfaces while still allowing investigation of general principles [2]. For example, restricted diffusion can limit the reactivity of molecules confined to a surface. A gas/liquid interface minimizes this problem, allowing studies to focus on the structure-directing elements of the reactants and surface. Analytical methods are available to probe structures directly at the air/water interface [3], but in addition, monolayers can be transferred from the water surface to solid supports using standard Langmuir–Blodgett (LB) film methods for more complete measurements of the structural and physical properties of the interface-formed assemblies.

We recently described [1] the synthesis of cyanide-bridged Fe^{III}–Ni^{II}, Fe^{III}–Co^{II}, and Fe^{III}–Mn^{II} square

* Corresponding author. Tel.: +1-352-392-9016; fax: +1-352-392-3255.

E-mail address: talham@chem.ufl.edu (D.R. Talham).

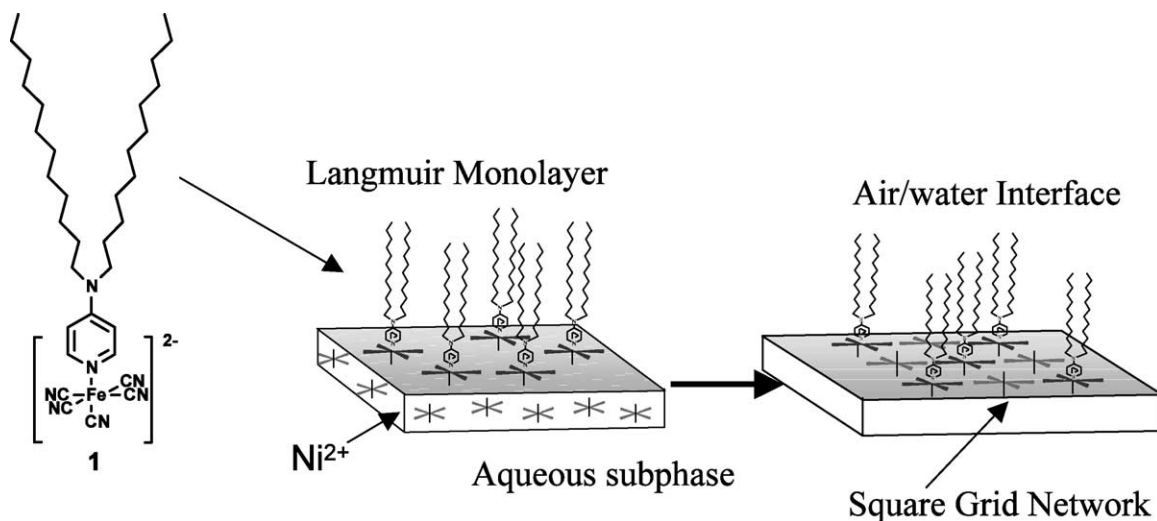


Fig. 1. Reaction of an amphiphilic pentacyanoferrate complex, **1**, confined to the air/water interface with aqueous Ni²⁺ ions results in a mixed-metal cyanide-bridged square grid network.

grid networks as monolayers at the air/water interface and their transfer to solid supports by the LB technique (Fig. 1). The two-dimensional networks can be transferred as an isolated monolayer, as a single bilayer, or as multiple bilayer assemblies (Fig. 2). DC magnetometry of transferred multilayer films showed the Fe–Ni film to be ferromagnetic [1a], consistent with related solid-state structures where Fe^{III} and Ni^{II} are bridged by cyanide ligands. The Fe–Co and Fe–Mn films are also magnetic [1b,1c].

In this paper, we demonstrate two applications of the interface-assembled networks, one of a fundamental nature and the other more practical. First, single-layer control of the deposition process provides an opportunity to observe how the magnetic properties of a film evolve as it changes from a monolayer to a bilayer to a multilayer film. The magnetic response is followed with

both DC and AC magnetometry. Second, monolayers can be transferred to a solid support to change the surface chemistry and provide epitaxy with solid-state molecule-based magnets. This surface modification process leads to the facile deposition of continuous thin films of Prussian blue related structures.

2. Experimental

2.1. LB film preparation and transfer

The mixed-metal cyanide square grid networks were prepared at the air/water interface as previously described [1]. For magnetic measurements, multilayer (FeNi-multi) and bilayer (FeNi-bi) films of the cyanide-bridged Fe^{III}Ni^{II} square grid network were prepared on

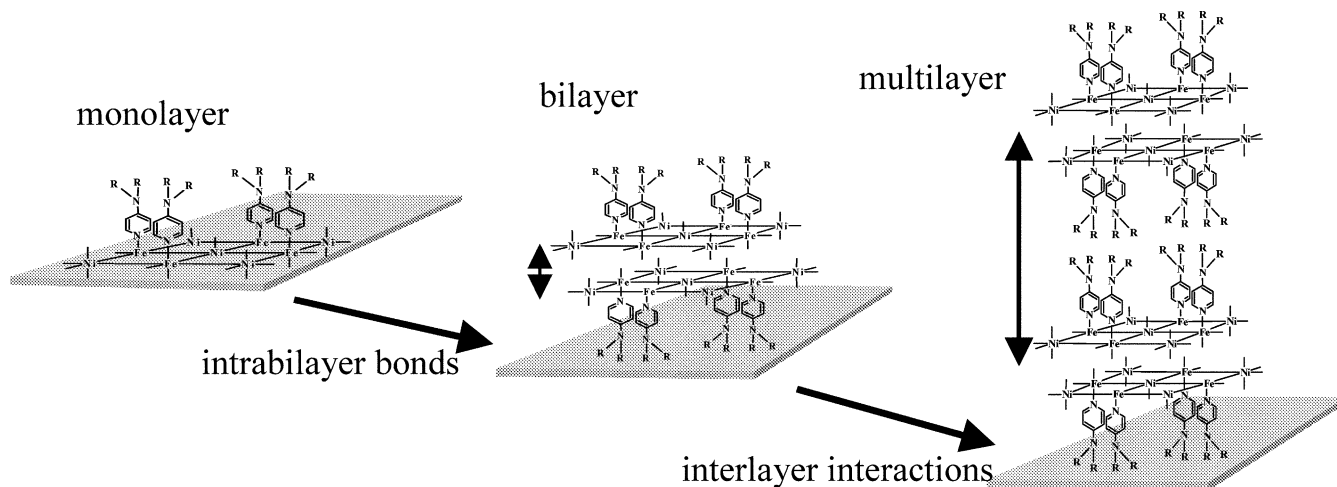


Fig. 2. Controlled transfer of the networks described in Fig. 1 to solid supports results in monolayer, bilayer, or multiple bilayer films. These films are used to monitor the evolution of magnetic properties as additional interactions are introduced.

Mylar and have also been described previously [1]. A sample consisting of a single monolayer (**FeNi-mono**) was prepared using a single transfer starting with the Mylar immersed in the subphase, i.e. hydrophilic transfer. The transfer ratio for **FeNi-mono** was $T_R = 1.0 \pm 0.1$. For the templating experiments, monolayers were transferred onto OTS-covered glass slides by starting with the substrate above the monolayer and transferring as the slide is immersed. The result is a hydrophobic transfer, and the slide is kept wet and used immediately.

2.2. Magnetization measurements

For magnetic measurements, each 10 cm² sample was cut and packed into gel caps for SQUID magnetometry. The rectangular pieces were packed parallel to one another and orientated with the plane of the sample surface aligned parallel (\parallel) or perpendicular (\perp) to the applied DC or AC magnetic fields. Background corrections were applied by subtraction of the diamagnetic signal measured on a similar (within 3%) mass of clean Mylar and sample container.

2.3. Instrumentation

Instrumentation for magnetic measurements and structural characterization were the same as described in earlier papers [1].

2.4. Formation of the Prussian blue films

The bulk Prussian blue film is assembled onto the templated substrate by a sequential deposition process. After transfer of the template layer by the LB method, the substrate was removed from the trough and rinsed briefly with water. The substrate was then immersed in the appropriate 0.01 M aqueous FeCl₂, Ni(NO₃)₂·6H₂O, or CrCl₂ solution for ~1 min, then rinsed twice by brief immersion in two separate beakers of nanopure water, then once by immersion in methanol, and finally dried under a stream of nitrogen before the process was repeated with an aqueous solution 0.01 M in the appropriate K₃Fe(CN)₆ or K₃Cr(CN)₆ complex salt. The Cr^{II}/[Cr^{III}(CN)₆] film was prepared under a N₂ atmosphere with N₂-purged solutions. A Cs_xK_(1-x)[Cr(CN)₆] solution 10 mM in CsNO₃ was used in the synthesis of the Ni^{II}/[Cr^{III}(CN)₆] film. One deposition cycle is comprised of one immersion, subsequently, in each of the metal ion solutions.

3. Results and discussion

3.1. Fabrication of monolayers, bilayers, and multilayers

The cyanide-bridged grid structures are formed when the amphiphilic pentacyanoferrate complex, **1**, is reacted at the air/water interface over a subphase containing the second metal ion, as illustrated in Fig. 1. The reactions can be monitored in situ at the air/water interface [1], and the resulting structure has been characterized in transferred films by grazing incidence X-ray diffraction and with IR, UV–Vis, and X-ray absorption spectroscopies [1]. The films can be deposited in different ways. Transfer onto a hydrophilic support yields a monolayer with the metal cyanide network in contact with the surface. Alternatively, if the monolayer is deposited onto a hydrophobic support, then the alkyl groups of the dialkylaminopyridine ligand are in contact with the solid surface and the metal cyanide network is directed away from it. Adding a second layer to this structure gives a bilayer, where two layers of the metal cyanide network are in contact, sandwiched between two layers of the organic groups. Continued deposition in this way leads to the buildup of multilayer films.

3.2. Evolution of magnetic properties

The Fe–Ni networks are ferromagnetic [1] and single-layer control over the deposition process provides an opportunity to observe how the magnetic properties of

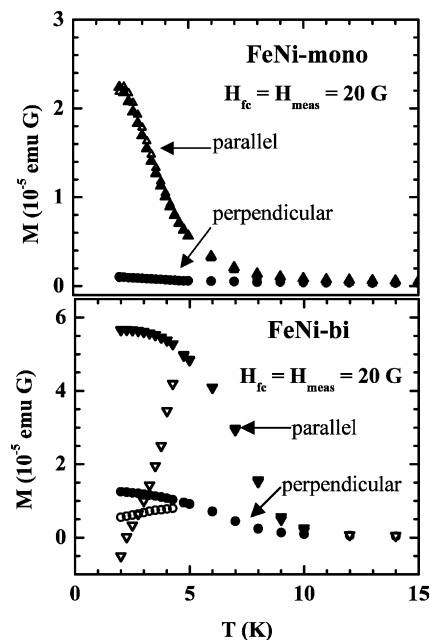


Fig. 3. Background-corrected magnetization vs. temperature for **FeNi-mono** and **FeNi-bi** in two orientations, parallel to the applied field and perpendicular to the applied field. Filled symbols are the field-cooled measurements and open symbols are zero-field-cooled. The measuring field is 20 G in each case.

the system evolve, as the film changes from a monolayer (**FeNi-mono**) to a bilayer (**FeNi-bi**) to multilayers (**FeNi-multi**). The DC magnetization of the **FeNi-mono** and **FeNi-bi** are compared in Fig. 3. In both films, the response is anisotropic, with larger magnetization when the films are oriented parallel to the applied field, reflecting the planar anisotropy of the network. The magnetization increases at higher temperature for the bilayer than for the monolayer, and the field-cooled and zero-field-cooled plots deviate near 5 K for the bilayer, indicating spontaneous magnetization. Spontaneous magnetization is not seen for the monolayer above 2 K.

The apparent ordering transition suggests the presence of coupling between the face-to-face networks within the bilayer, an interaction that is absent in the monolayer (Fig. 2). The interaction is most likely covalent in nature, brought about through bridging of the axial cyanide of some number of the amphiphilic pentacyanoferrate complexes to available coordination sites on nickel ions in the adjacent network. This covalent bonding arrangement would favor ferromagnetic exchange by the same mechanism that promotes ferromagnetism within one network plane [4–6]. Magnetization measurements up to 30 T on multiple bilayer samples showed no evidence for ferrimagnetic or metamagnetic behavior [7], supporting the assignment of ferromagnetic coupling within the bilayers.

The temperature dependence of the magnetization for the multilayer sample, **FeNi-multi**, is almost identical to that of the bilayer. Both samples are anisotropic and

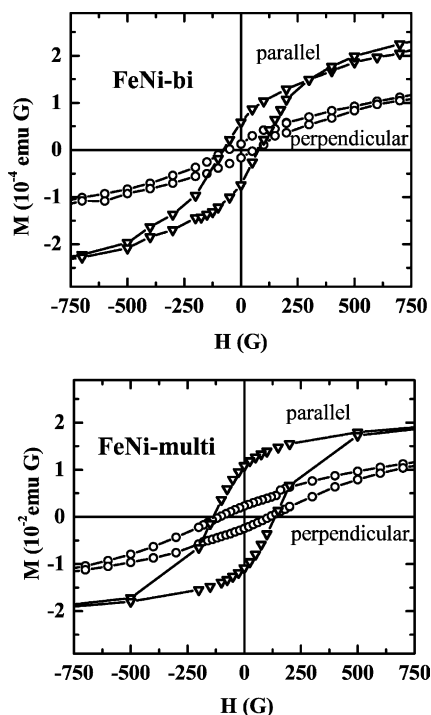


Fig. 4. Background-corrected magnetization vs. field at 2 K for **FeNi-bi** and **FeNi-multi** in parallel and perpendicular orientations.

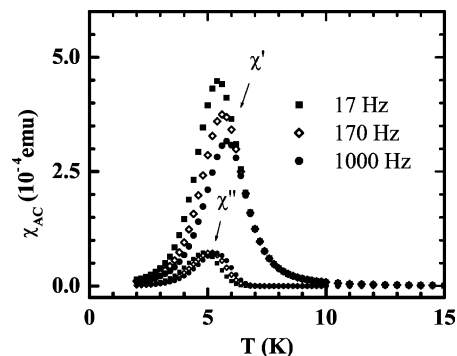


Fig. 5. Background-corrected AC susceptibility for **FeNi-multi** at three frequencies. Data are acquired with the film parallel to the applied field with an AC field of 4 G.

show a divergence of the field-cooled and zero-field-cooled plots at the same temperature. However, there is a difference in the magnetization vs. field plots (Fig. 4). The hysteresis is larger for the multilayer film, $H_c = 135$ G, than for the bilayer, $H_c = 75$ G. Overall, the data suggest an additional interaction that is not present in the bilayer. Adjacent bilayers are not linked covalently, so interbilayer interactions are likely dipolar in nature. Dipolar interactions over similar distances have been proposed to play a significant role in solid-state examples of organic/inorganic layered ferromagnets [8].

Measurements of the AC susceptibility for each sample show pronounced frequency dependence, indicating spin glass-like behavior. The AC data for **FeNi-multi** is shown in Fig. 5. A spin glass state can be distinguished from a superparamagnet by quantifying the frequency dependence through the ratio ϕ [9], which may be written as

$$\phi = \frac{\Delta T_f}{T_f \Delta(\log \omega)} \quad (1)$$

where T_f is the temperature at which the maximum in $\chi'(T)$ occurs, ΔT_f the difference in T_f between an initial frequency ω and final frequency ω_f , and $\Delta(\log \omega)$ the difference between the log of the initial and final measuring frequencies. The values of ϕ obtained for **FeNi-bi** and **FeNi-multi** are 0.05 and 0.04, respectively, which fall within the range typical for insulating spin glasses [9] and are very similar to those reported by Buschmann et al. [10] for a series of hexacyanomanganate Prussian blue analogues. A somewhat larger value of $\phi = 0.10$ was obtained for **FeNi-mono**, which falls between the values typical of superparamagnets and spin glasses [9], so the ferromagnetic domains are more weakly interacting in the monolayer than in the bilayer or multilayer.

The changing interactions, as the films are built-up from a monolayer to multiple bilayers, are summarized in Fig. 2. Additional layers add additional interactions, which are evident in the magnetic responses. The system

may be described as a progression from moderately interacting ferromagnetic domains in the monolayer to a collective more strongly interacting glass-like state in the bilayer and multilayer films.

3.3. Templating films of solid-state molecule-based magnets

In a more practical application of the monolayer networks, they can be used to derivatize a surface, changing its chemistry. The specific example to be discussed here is use of the monolayer to provide epitaxy with a molecule-based magnetic solid, so that deposition of a thin film of the solid becomes easier and gives better surface coverage. The $\text{Fe}^{\text{III}}\text{-Ni}^{\text{II}}$ cyanide-bridged two-dimensional square grid network described in Fig. 1 has lattice parameters [1] that are nearly the same as the (100) face of Prussian blue and related mixed-metal derivatives [11], so we can use it to template the growth of different hexacyanometallates. Prussian blue related films are of interest for applications in photovoltaics [12], electrochromics [13], and sensing [14], in addition to their magnetic properties [15]. However, the low solubility and poor crystallinity of most derivatives make surface wetting and the fabrication of continuous films difficult. By providing a surface layer with similar chemistry and epitaxy, continuous films can be formed.

Our method for preparing thin metal cyanide films is outlined in Fig. 6. It is modeled after the layer-by-layer deposition process commonly used to form polyelectrolyte multilayer films and similar to the approach taken by Pyrasch and Tieke [16]. Fig. 6 is specific to the preparation of a Prussian blue film, but the method itself is general and various combinations of aqueous metal salts and hexacyanometallate complexes can be substituted for the $\text{Fe}_{\text{aq}}^{3+}$ and $[\text{Fe}(\text{CN})_6]^{4-}$ ions depicted in the scheme. An $\text{Fe}^{\text{III}}\text{-Ni}^{\text{II}}$ monolayer is used as the template. The cubic Prussian blues all have similar lattice constants, so the lattice matching with the overlayer does not change much with the identity of the metal ions in the template.

Fig. 7 is an AFM image of a Prussian blue film formed from FeCl_2 and $\text{K}_3\text{Fe}(\text{CN})_6$ after five deposition cycles. The image shows complete surface coverage over the $100\ \mu\text{m}^2$ image. The higher regions in the film are due to smaller crystallites on the surface and indicate that film growth is not purely layer-by-layer, but that crystallites form once growth is initiated. However, AFM images also confirm that the metal cyanide completely covers the surface. Even the low spots are the Prussian blue films and these can be verified when defects are found in the film. Further evidence that the surface coverage is complete in these films is provided by SEM images. An SEM image taken of an

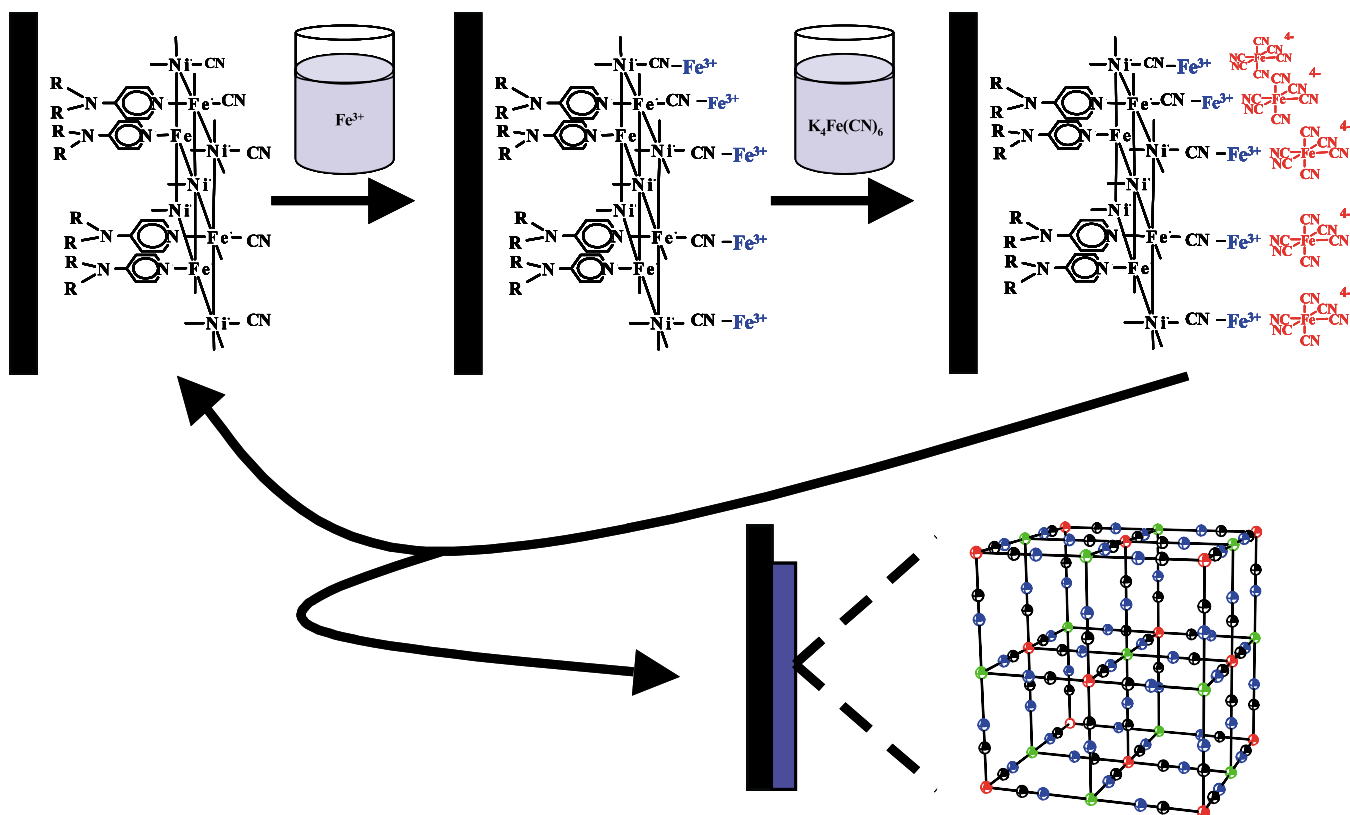


Fig. 6. The sequential deposition of cationic and anionic building blocks to form Prussian blue at a surface modified with a monolayer of a square grid template.

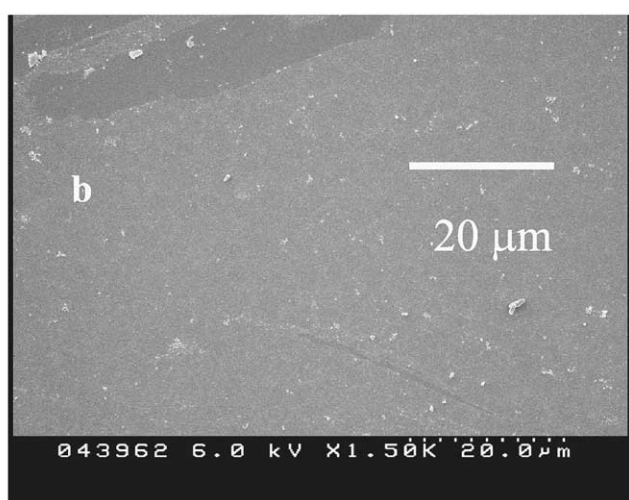
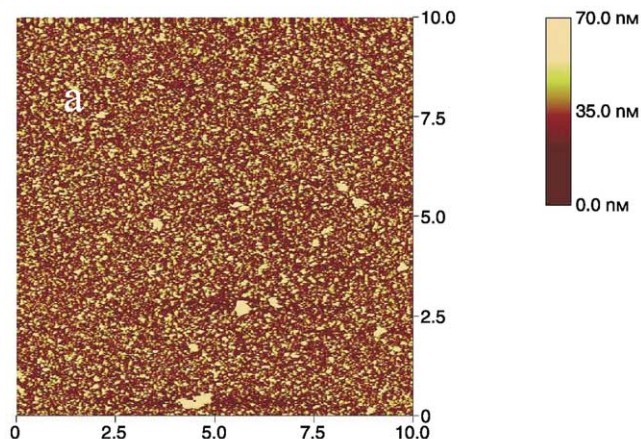


Fig. 7. AFM image of a Prussian blue film after three deposition cycles (top). SEM image of a Prussian blue film after 10 cycles (bottom). Both films are deposited on glass.

$\text{Fe}^{\text{III}}/[\text{Fe}^{\text{II}}(\text{CN})_6]$ film after 10 cycles is also shown in Fig. 7. The abrasion in the upper left corner clearly shows the substrate below a Prussian blue film that is continuous over the remaining $400 \mu\text{m}^2$.

The Prussian blue film is magnetic. Solid-state Prussian blue is a known ferromagnet with $T_c = 5.6 \text{ K}$ [17] and similar response is observed in the thin film samples. Data for a 10 cm^2 film after 100 deposition cycles are shown in Fig. 8, where the field-cooled magnetization rapidly increases near 5 K.

Similar results were obtained on the other metal cyanide films. A film with nominal formula $\text{Cs}_7\text{Ni}_k^{\text{II}}[\text{Cr}^{\text{III}}(\text{CN})_6]_l$ prepared from $\text{Ni}(\text{NO}_3)_2 \cdot 6\text{H}_2\text{O}$ and $\text{K}_3\text{Cr}(\text{CN})_6$ in the presence of CsNO_3 is shown in the SEM image of Fig. 9. Magnetization data for an 8 cm^2 film after 20 deposition cycles are also shown in Fig. 9. The ferromagnetic ordering temperature, $T_c = 75 \text{ K}$, extracted from $M_{\text{fc}}(T)$ data is slightly lower than $T_c = 90 \text{ K}$ reported for the bulk solid [18]. Ordering temperatures of the hexacyanometallates are known to be sensitive to the precise stoichiometry and are often

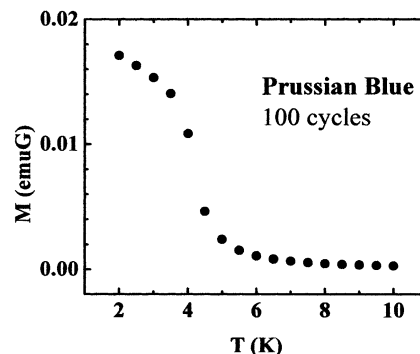


Fig. 8. Magnetization vs. temperature of a templated Prussian blue film.

affected by the identity of the counterion [18]. Since the structural coherence of the film was confirmed by X-ray diffraction, the lower ordering temperature observed in the film most likely reflects a lower Ni:Cr ratio in the film relative to the solid-state material. The film displays a clear hysteresis at 5 K with an H_c of 70 G and a remnant magnetization (M_{rem}) 50% of the saturation value. Both of these values are very similar to those reported by Gadet [18a] for the solid analogue.

4. Conclusions

These experiments demonstrate that the metal cyanide square grid network monolayers can be transferred to a solid support to facilitate subsequent deposition from solution of mixed-metal Prussian blue related films. The combination of the right surface chemistry with appro-

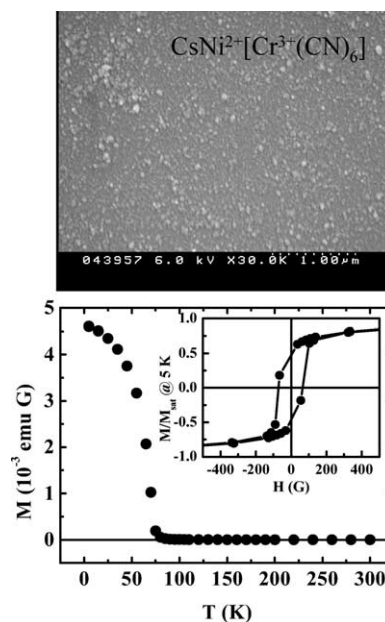


Fig. 9. SEM image of $\text{Ni}^{\text{II}}/[\text{Cr}^{\text{III}}(\text{CN})_6]$ after 10 cycles (top). Magnetization vs. temperature and magnetization vs. field for $\text{Ni}^{\text{II}}/[\text{Cr}^{\text{III}}(\text{CN})_6]$ after 20 cycles (bottom).

appropriate lattice matching helps the molecule-based magnetic solid to wet the surface to give continuous films. Two examples, the iron-based Prussian blue and a related $\text{Ni}^{\text{II}}/[\text{Cr}^{\text{III}}(\text{CN})_6]$ film, are demonstrated here and current work is exploring other compositions.

The metal cyanide monolayers have also been used in a more fundamental study. The ability to regulate the monolayer transfer leads to films with a controlled number of layers. By preparing monolayer, bilayer, and multiple bilayer samples, we are able to quantify how magnetic interactions change in films with different architectures.

Acknowledgements

This research was supported by the National Science Foundation through grant DMR-9900855 (DRT) and by the American Chemical Society through grant ACS-PRF-36163-AC5 (MWM, DRT). Use of the Advanced Photon Source was supported by the US Department of Energy, Office of Science, Office of Basic Energy Sciences, under Contract No. W-31-109-ENG-38. We also acknowledge support from the Materials Research Collaborative Access Team (MRCAT) at the Advanced Photon Source and the Electron Microscopy Core Laboratory, Biotechnology Program, University of Florida.

References

- [1] (a) J.T. Culp, J.-H. Park, D. Stratakis, M.W. Meisel, D.R. Talham, *J. Am. Chem. Soc.* 124 (2002) 10083;
(b) J.T. Culp, J.-H. Park, M.W. Meisel, D.R. Talham, *Polyhedron*, in press;
(c) J.T. Culp, Ph.D. Thesis, University of Florida, 2002.
- [2] (a) J. Michl, T.F. Magnera, *Proc. Natl. Acad. Sci.* 99 (2002) 4788;
(b) N. Varaksa, L. Pospilil, T.F. Magnera, J. Michl, *Proc. Natl. Acad. Sci.* 99 (2002) 5012.
- [3] I. Kuzmenko, H. Rapaport, K. Kjaer, J. Als-Nielsen, I. Weissbuch, M. Lahav, L. Leiserowitz, *Chem. Rev.* 101 (2001) 1659.
- [4] S. Ferlay, T. Mallah, R. Ouahes, P. Veillet, M. Verdaguer, *Nature* 378 (1995) 701.
- [5] (a) M. Ohba, H. Okawa, T. Ito, A. Ohto, *Chem. Commun.* (1995) 1545;
(b) M. Ohba, H. Okawa, N. Fukita, Y. Hashimoto, *J. Am. Chem. Soc.* 119 (1997) 1011.
- [6] S. Juszczuk, C. Johansson, M. Hanson, A. Ratuszna, G. Malecki, *J. Phys.: Condens. Matter* 6 (1994) 5697.
- [7] J.-H. Park, J.T. Culp, D.W. Hall, D.R. Talham, M.W. Meisel, *Physica B*, in 329–333 (2003) 1152.
- [8] V. Laget, C. Hornick, P. Rabu, M. Drillon, R. Ziessel, *Coord. Chem. Rev.* 180 (1998) 1533.
- [9] J.A. Mydosh, *Spin Glasses*, Taylor & Francis, Washington, DC, 1993.
- [10] (a) W.E. Buschmann, J. Ensling, P. Gutlich, J.S. Miller, *Chem. Eur. J.* 5 (1999) 3019;
(b) W.E. Buschmann, J.S. Miller, *Inorg. Chem.* 39 (2000) 2411.
- [11] A. Ludi, H.U. Güdel, *Struct. Bonding* 14 (1973) 1.
- [12] G.R. Torres, E. Dupart, C. Mingotaud, S. Ravaine, *J. Phys. Chem.* 104 (2000) 9487.
- [13] (a) R.J. Mortimer, *Chem. Soc. Rev.* 26 (1997) 147;
(b) K. Itaya, I. Uchida, V.D. Neff, *Acc. Chem. Res.* 19 (1986) 162.
- [14] (a) J.J. Xu, H.Q. Fang, H.Y. Chen, *J. Electroanal. Chem.* 426 (1997) 139;
(b) S. Bharathi, V. Yegnaraman, G.P. Rao, *Langmuir* 11 (1995) 666;
(c) K. Itaya, T. Ataka, S. Toshima, *J. Am. Chem. Soc.* 104 (1982) 4767.
- [15] (a) C. Lafuente, C. Mingotaud, P. Delhaes, *Chem. Phys. Lett.* 302 (1999) 523;
(b) C. Mingotaud, C. Lafuente, J. Amiel, P. Delhaes, *Langmuir* 15 (1999) 289;
(c) W.E. Buschmann, S.C. Paulson, C.M. Wynn, M.A. Girtu, A.J. Epstein, H.S. White, J.S. Miller, *Chem. Mater.* 10 (1998) 1386.
- [16] M. Pyrasch, B. Tiede, *Langmuir* 17 (2001) 7706.
- [17] F. Herren, P. Fischer, A. Ludi, W. Halg, *Inorg. Chem.* 19 (1980) 956.
- [18] (a) V. Gadet, T. Mallah, I. Castro, M. Verdaguer, P. Veillet, *J. Am. Chem. Soc.* 114 (1992) 9213;
(b) M. Verdaguer, A. Bleuzen, V. Marvaud, J. Vaissermann, M. Seuleiman, C. Desplanches, A. Scullier, C. Train, R. Garde, G. Gelly, C. Lomenech, I. Rosenman, P. Veillet, C. Cartier, F. Villain, *Coord. Chem. Rev.* 192 (1999) 1023.